AEM
Journals.ASM.org

Fluid Flow Induces Biofilm Formation in *Staphylococcus epidermidis* Polysaccharide Intracellular Adhesin-Positive Clinical Isolates

Westbrook M. Weaver,[a,b] Vladana Milisavljevic,[c] Jeff F. Miller,[d] and Dino Di Carlo[a,b]

Department of Biomedical Engineering, University of California, Los Angeles, Los Angeles, California, USA[a]; California NanoSystems Institute, University of California, Los Angeles, Los Angeles, California, USA[b]; Department of Pediatrics, Division of Neonatology and Developmental Biology, David Geffen School of Medicine, University of California, Los Angeles, Los Angeles, California, USA[c]; and Department of Microbiology, Immunology, and Molecular Genetics (MIMG), David Geffen School of Medicine, University of California, Los Angeles, Los Angeles, California, USA[d]

***Staphylococcus epidermidis* is a common cause of catheter-related bloodstream infections, resulting in significant morbidity and mortality and increased hospital costs. The ability to form biofilms plays a crucial role in pathogenesis; however, not all clinical isolates form biofilms under normal *in vitro* conditions. Strains containing the *ica* operon can display significant phenotypic variation with respect to polysaccharide intracellular adhesin (PIA)-based biofilm formation, including the induction of biofilms upon environmental stress. Using a parallel microfluidic approach to investigate flow as an environmental signal for *S. epidermidis* biofilm formation, we demonstrate that fluid shear alone induces PIA-positive biofilms of certain clinical isolates and influences biofilm structure. These findings suggest an important role of the catheter microenvironment, particularly fluid flow, in the establishment of *S. epidermidis* infections by PIA-dependent biofilm formation.**

Staphylococcus epidermidis is a normal inhabitant of human skin and mucous membranes and is currently a leading cause of health care-associated infections (HAIs) (15). This organism is a prominent colonizer of implanted polymer devices, including intravascular catheters (21). Catheter-related bloodstream infections (CRBSIs) are a significant cause of morbidity and mortality in hospitalized patients, especially those with underdeveloped or weakened immunity (3).

Biofilm formation appears to be a key component in the pathogenesis of infections caused by *S. epidermidis*. Previous reports suggest that there is a preferential ability of certain strains of *S. epidermidis* to cause infection and that biofilm formation is a promising therapeutic target for CRBSI (4, 16, 17). Many *S. epidermidis* biofilms are largely composed of the polysaccharide intercellular adhesin (PIA), a poly-β-1,6-*N*-acetylglucosamine (10), production of which is associated with the upregulation of the chromosomal *icaADBC* gene cluster (6). *S. epidermidis* isolates display strain-to-strain variation in PIA-dependent biofilm production. The two main groups are those lacking the *ica* locus, which are unable to form PIA-based biofilms, and those containing *ica* genes (*ica*$^+$). Within the *ica*$^+$ group are strains that constitutively secrete PIA (biofilm^c), strains that do not produce PIA under any *in vitro* conditions that have been tested (biofilm$^-$), and strains that can be induced (biofilm^i) to secrete PIA by exposure to alcohols (thought to simulate a heat shock-like response by unfolding native proteins) or osmotic stressors, such as NaCl (1, 7, 8). It is important to note that some clinically isolated strains have been shown not to fit in these categories. Specifically, there are those that lack the *ica* locus and are still able to form biofilms after significantly longer culture periods than those for the *ica*$^+$ strains (2, 12), as well as *ica*$^+$ strains that have the insertion sequence IS*257* in *icaA* (13, 14). These biofilms contain primarily proteinaceous, rather than PIA-based, matrices. In our clinical isolates, however, biofilm formation is PIA mediated.

The catheter microenvironment, in which biofilm formation is key for establishing infection, is an inherently mechanical environment characterized by fluid flow and shear stress. To better understand the role of these fluid-induced stresses on biofilm formation, we used a parallel microfluidic device (23) that directs planktonic cell adhesion to isolated chambers within microchannels (red in Fig. 1A and B) and subsequently exposes multiple sessile populations of bacteria to well-defined fluid flows and shear stresses in a single experiment, with no cross talk between shear stress chambers connected in parallel (Fig. 1C; see also Fig. S2E in the supplemental material). The shear stresses applied in the microfluidic biofilm assay ranged from 0.065 to 1.14 Pa in a single experiment (Fig. 1D; see also Fig. S2D in the supplemental material), representing wall shear stresses present in capillaries and venules (between 0.05 Pa and 4 Pa) (5, 9) and catheter lumens (0.02 to 3 Pa in a typical 1.9 French catheter). The spectrum of shear forces acting in catheters under normal operating conditions of flow rates from 1 to 10 ml/h was determined using fluid flow models of both single and double lumen catheter sections that we created using COMSOL Multiphysics (see Fig. S1 in the supplemental material). We investigated a variety of clinical isolates of *S. epidermidis* to determine the potential variation in PIA-based biofilm formation in response to clinically relevant fluid forces experienced by *S. epidermidis* during pathogenesis.

MATERIALS AND METHODS

Bacterial strains and culture conditions. Two ATCC strains representing *S. epidermidis* lacking *ica* (12228) and containing *ica* (35984 or RP62A) were used as negative and positive controls, respectively, for PIA-based biofilm formation. Five clinical isolate strains previously isolated and described by Milisavljevic et al., all containing the *ica* locus and representing

Received 10 April 2012 Accepted 7 June 2012
Published ahead of print 15 June 2012
Address correspondence to Vladana Milisavljevic, vmilisavljevic@mednet.ucla.edu.
Supplemental material for this article may be found at http://aem.asm.org/.

doi:10.1128/AEM.01139-12

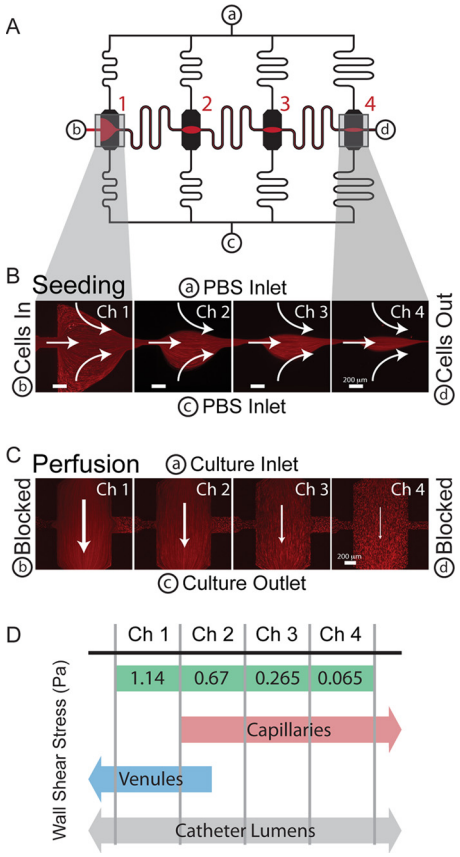

FIG 1 Schematic and operation of the microfluidic biofilm assay. (A) The microchannel design consists of 4 parallel channels (black) with culture chambers placed halfway between inlet a and outlet c. These are connected by a seeding channel (red and black) from b to d. (B) Prior to shear culture, cells are seeded in the device by creating pinched flow in each chamber. (C) Subsequently, b and d are blocked, and the channels are converted to perfusion mode, in which chamber 1 (Ch1) has the lowest resistance and highest wall shear stress. There is significantly lower flow in the seeding channels per the design of the device. Red streaks in panels B and C are 1-μm fluorescent polystyrene beads in flow. (D) The wall shear stress spans over an order of magnitude in a single experiment, covering ranges seen in capillaries and venules as well as those calculated for catheter lumens. Shear stresses presented are for an inflow of 18 μl/min.

distinct PIA-forming biofilm phenotypes, were also used (11). The PIA-negative group is represented by strain A-10, the constitutive PIA-based biofilm formers are represented by A-26, and the inducible strains are represented by A-5, W-166, and Z-173.

Bacteria were grown in an overnight culture in tryptic soy broth with 2.5% glucose (Sigma) in a shaking incubator at 240 rpm and 37°C. Frozen stocks were kept at −80°C in 25% glycerol and streaked onto 1.5% tryptic soy agar (Sigma). Isolated colonies were subsequently picked for overnight broth culture prior to biofilm experiments and grown to an optical density at 600 nm (OD_{600}) of 0.6 before being washed with phosphate-buffered saline (PBS) and resuspended 1:10 in PBS prior to inoculation in the microfluidic biofilm assay.

Microtiter plate assays. Semiquantitative microtiter plate assays for biofilm formation were performed as previously reported (11). Overnight cultures grown in tryptic soy broth (TSB; Becton Dickenson) were diluted 1:100 in culture medium, and 200 μl was plated in a flat-bottom polystyrene 96-well plate (Greiner Bio). For experiments using EtOH induction, overnight cultures were diluted 1:100 in culture medium containing 1 to 4% (vol/vol) EtoH and grown for 12 h. Subsequently, these subcultures were diluted 1:100 in the respective induction medium and plated in triplicate in well plates as described above. Biofilms were grown for 24 h and then washed with sterile water, fixed with methanol (Sigma), and stained with 2% crystal violet (Sigma). Well absorbance was measured at 570 nm using a plate reader system (Tecan Infiniti F200). Fold increases in biofilm in these experiments were presented as a ratio of the well absorbance to that of the negative-control wells in which no bacteria were seeded.

Microfluidic biofilm assays. A more detailed description of how devices were fabricated and how channels were prepared for culture can be found in the supplemental Materials and Methods.

The device utilized for this study operates in two modes: (i) seeding of bacteria in a pattern to areas of known shear and (ii) subsequent exposure of isolated populations of sessile bacteria to shear. All flow is achieved using a syringe pump (Harvard apparatus) and plastic syringes (Becton Dickenson), connected to devices using PEEK tubing (Upchurch Scientific) and luer lock stubs (Fisher).

Prior to seeding, channels were converted to a hydrophobic state by utilizing a slight modification of our previously published method of *in situ* silane chemistry (23), using an octyl(tri-ethoxy)silane (OTES).

Bacteria were seeded in a specific pattern within the device by using a modification of the functionalization setup previously described (23). Briefly, devices were preequilibrated with phosphate-buffered saline (PBS) (pH 7.4) prior to seeding bacteria in the chambers. To seed, bacteria were injected into inlet b, while PBS was injected into inlets a and c. Seeding was performed for 1 h, and then the device was converted to perfusion mode by blocking inlet b and outlet d. Perfusion was carried out in a 37°C incubator, with flowing TSB with 2.5% glucose at 18 μl/min for high-flow-rate devices and at 4.5 μl/min for low-flow-rate devices.

After perfusion for 6, 12, or 24 h, biofilms in the microfluidic assay were first washed at 4°C with PBS at 18 μl/min or 4.5 μl/min for 20 min and then fixed by flowing through 400 μl of 4% paraformaldehyde at the respective flow rate used for the culture. The devices were incubated at 4°C for 12 h and then washed with 400 μl of PBS at 10 μl/min.

PDMS/glass milliwell plate assays. Polydimethylsiloxane (PDMS)/glass millimeter-scale wells were created to allow culture of biofilms without flow while maintaining the same substrate materials and surface modifications present in the microfluidic devices. These wells were constructed by pouring thin (~5-mm) strips of PDMS. Wells were punched in these strips using a 1-mm-diameter biopsy punch, and the wells were bonded to 18-mm-diameter glass coverslips (Fisher) using O_2 plasma, resulting in wells with an ~5-μl volume. These wells were then placed in the bottom of a 12-well flat-bottom plate (Greiner Bio). Bacteria were seeded in these wells by washing overnight cultures (OD_{600} = 0.6) 3 times in PBS and resuspending 1:10 in PBS. Wells were seeded for 1 h, and then the well plates were aspirated, washed with PBS, and filled with either TSB or TSB supplemented with 4% (vol/vol) EtOH.

Collection of cells from the microfluidic biofilm assay after culture. To collect cells after culture within the microfluidic device, cells were physically excised. To accomplish this, devices were disconnected from medium flow after 24 h of culture and the outside surfaces of the devices were washed with 70% EtOH and dried using a Kimwipe. A razor scalpel was flame sterilized and used to cut out a hole in the PDMS above each chamber in the device (see Fig. S4A in the supplemental material). A sterile 10-μl pipette tip was used to scrape cells from the exposed chamber inner surfaces, and these cells were streaked onto tryptic soy agar plates and grown at 37°C for 18 h. Single colonies were picked from these plates and used for further screening using microtiter plate assays.

Fluorescent staining of biofilms. All staining was performed in 4°C using a flow rate of 10 μl/min for total volumes of 400 μl for microfluidic staining and by adding 5 μl of solution to the milliwells. PIA was stained for 3 h using a 100-μg/ml solution of fluorescein isothiocyanate (FITC)-labeled wheat germ agglutinin (WGA) (Sigma) in PBS (pH 7.4) with 0.5% bovine serum albumin (BSA). Bacterial cells were stained using 4′,6-diamidino-2-phenylindole (DAPI) (Sigma) and ethidium homodimer I

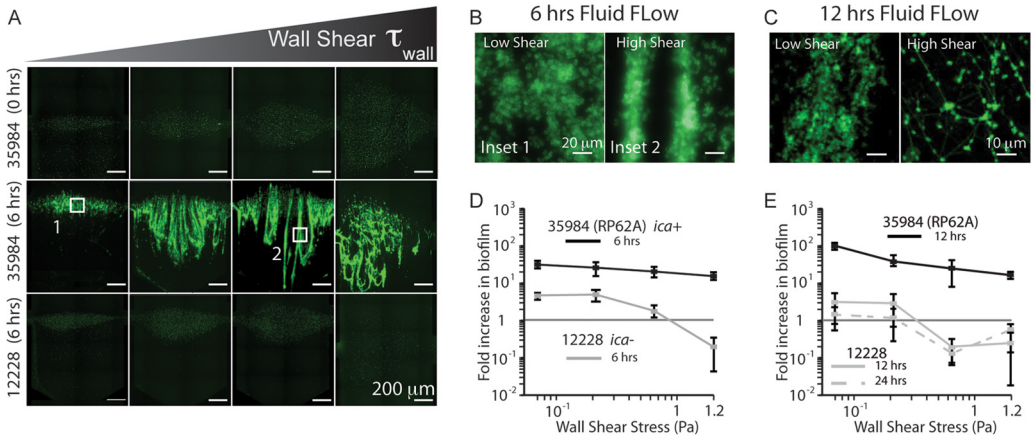

FIG 2 *S. epidermidis* ATCC strains are distinguishable by biofilm phenotype when grown under flow. (A) Panels showing the fluorescence from WGA staining both before shear (0 h) and after 6 h of shear for 35984 (*ica*$^+$, biofilm^c), and 12228 (lacking *ica*, biofilm$^-$). (B) Higher-magnification images (×40) illustrate the architectural differences between 35984 biofilms grown under different shear stresses. Higher shear results in streamer formation. (C) CLSM images (magnification, ×63) of 35984 biofilms after 12 h of shear indicate that these differences are enhanced over time (green, PIA). (D) Quantification of the subpanels in panel A, showing measurable differences in biofilm phenotype after 6 h. (E) Quantitative differences continue after 12 and 24 h of culture. 12228 decreases at high shear, indicating a release of cells from the surface, and maintains the initial inoculum levels at lower shears, while 35984 flourishes at all shear stresses.

(EtHDI) (Invitrogen) diluted to 1 μg/ml in PBS containing 1% ascorbic acid. Biofilms were stained for 30 min with DAPI and EtHDI and then visualized using a Nikon Ti inverted wide-field fluorescence microscope with a quantitative grayscale cooled charge-coupled device (CCD) camera (Coolpix) or a Nikon A1 confocal laser scanning microscope (CLSM).

Crystal violet staining in microtiter plates detected biofilm irrespective of matrix composition, whereas in the microfluidic assay, we stained specifically for PIA. As those strains able to form biofilms in microtiter assays directly correspond to those stained specifically for PIA, this indicated biofilms including a significant PIA fraction, and PIA staining was used as a surrogate for biofilm formation.

Image analysis. Fold increase in the area stained by FITC-WGA was used to quantify biofilm accumulation in microfluidic assays and Milliwell plate assays. To obtain these values, images were taken at the same exposure time (1 s) under a ×20 magnification using an extra-long working distance dry Nikon objective. Each chamber in the microfluidic biofilm assay was captured by taking 20 images and stitching them together (5 wide by 4 high).

Using a postprocessing intensity thresholding algorithm in the Nikon Advanced Research software package (version 3.2), pixel areas with intensity values above a threshold (corresponding to the biofilm matrix) within the chamber are quantified and presented as a ratio to the areas stained by FITC-WGA immediately after seeding prior to perfusion (example images are shown in the panels in Fig. 2A). There is a background level of staining for non-biofilm-forming strains that is likely due to the polysaccharides on the cell surface; however, biofilm and cells not forming biofilm are still well resolved. Fold increases of <1 indicate a reduction in the number of cells on the surface, increases of between 1 and 5 indicate cell growth, and increases of >5 indicate biofilm production.

Statistical analysis. All statistical tests were performed using variations on the Student *t* test. To compare different conditions and/or strains, the *t* test comparing two populations of unequal variances was used. To determine if any condition led to significant biofilm induction (compared to 1), *t* tests comparing a population to a specified value were used. All data are presented as averages of at least three experiments, with all error bars showing standard deviations of the mean.

RESULTS

***S. epidermidis* isolates represent three biofilm phenotypes.** Using conventional microtiter plate assays, we verified that the strains used in this study represent the three main biofilm phenotypes. Clinical strain A-26 (*ica*$^+$, biofilm^c) formed strong biofilms under standard conditions, similar to ATCC 35984, whereas strains A-10 (*ica*$^+$, biofilm$^-$) and ATCC 12228 were unable to form biofilms, irrespective of culture conditions (see Fig. S3A in the supplemental material). Strains A-5, W-166, and Z-173 (*ica*$^+$, biofilm^i) were all induced to form biofilms upon supplementation of the medium with ethanol (see Fig. S3B in the supplemental material).

PIA-positive biofilms are formed under flow by an *ica*$^+$ ATCC strain. After culturing bacteria under fluid flow for 6 h, the constitutive ATCC strain 35984 produced PIA-positive biofilms across all shear levels, while the ATCC 12228 strain lacking *ica* produced no biofilms at any shear (Fig. 2A). Biofilm was quantified as the ratio of the chamber area stained by WGA to the baseline just after seeding and prior to exposure to shear, presented as a fold increase in Fig. 2D. This measurement reflects biofilm accumulation in each chamber respective to that chamber's initial condition and accounts for the differences in seeding pattern shapes between chambers that result from fluid flow during seeding (see Fig. S2A in the supplemental material). To characterize initial conditions in our microfluidic channels, we demonstrated that although the patterns were different sizes (see Fig. S2B in the supplemental material), the surface densities of the bacteria remained the same, averaging 1 CFU for every 2 μm^2 (see Fig. S2C in the supplemental material).

Due to nonzero staining of 12228, our metric of fold increase in the area stained by WGA allowed measurement of the amount of cells present on channel surfaces after shear. Figure 2D indicates that 12228 cells were able to multiply on the surface at low shear, but numbers actually decreased over time at higher shear (fold increases of <1), indicating that cells were detached from surfaces under these conditions.

PIA biofilms produced by the constitutive strain 35984 at low fluid flow displayed an isotropic structure (Fig. 2B, inset 1). In contrast, higher shear resulted in biofilms with aligned PIA streamers of ~20 μm in width extending in the direction of flow (Fig. 2B, inset 2) and loop structures under the highest shear (Fig.

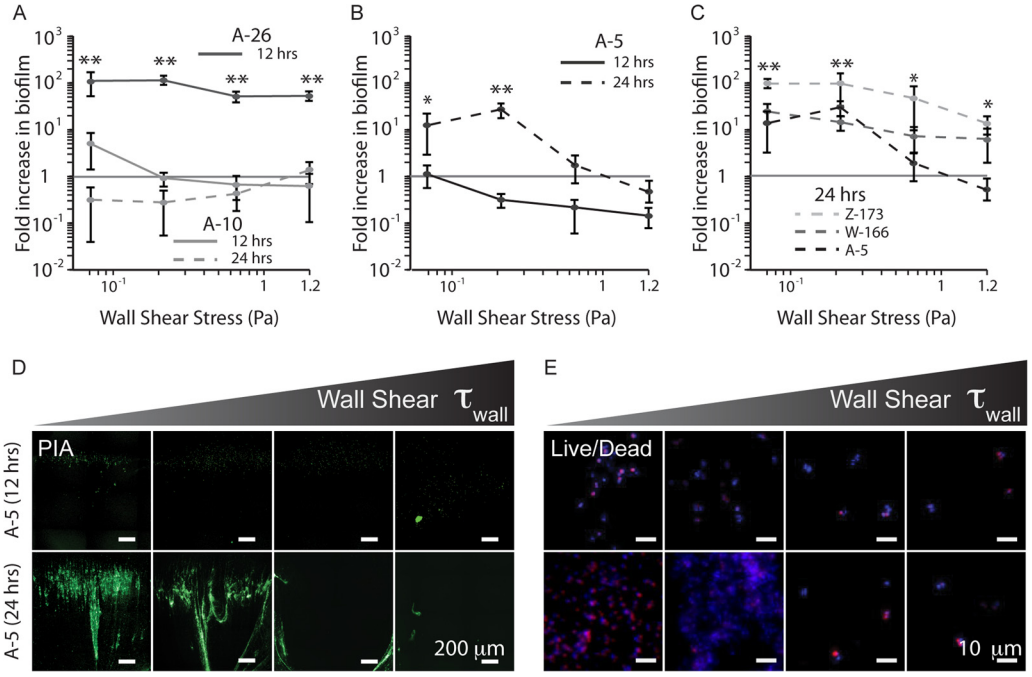

FIG 3 Fluid flow results in differential biofilm formation among clinical isolates. (A) Strain A-26 forms strong biofilms under all shear stresses, whereas A-10 is unable to form biofilms under any shear after 24 h. (B) Strain A-5, after a lag phase of at least 12 h, forms significant biofilm when exposed to fluid flow and shear, with the most biofilm at 0.26 Pa. (C) Strains W-166 and Z-173 are able to form biofilms under a broader range of flow rates than A-5. (D) WGA staining of the biofilm matrix for A-5 after 12 and 24 h of culture under flow. (E) Live/dead staining of the same time points from panel D, showing live cells present on the channel surface after 12 h. These cell numbers drastically increase after 24 h. One asterisk indicates a *P* value of <0.01 and two asterisks indicate a *P* value of <0.005 measured against 1. Green, PIA; blue, DAPI; red, EtHDI.

2A). These architectural differences in shear-dependent biofilm formation became more evident with increasing time. After 12 h of culture, large (~40-μm) streamers formed at low shear and a web-like PIA matrix architecture connecting small, dense colonies was observed at high shear (Fig. 2C).

Over culture periods of 12 and 24 h, 35984 continued to produce substantial biofilms across the spectrum of fluid flow, while, as expected, 12228 did not form biofilms (Fig. 2E). Using our microfluidic device, we were able to quantitatively measure the phenotype of biofilm formation under flow for these well-characterized ATCC strains with high confidence (*P* value of <0.01 for all shear stresses when comparing 35984 and 12228). These results laid the groundwork for assays using clinical isolates with a broader range of biofilm phenotypes.

PIA-positive biofilm formation in clinical isolates under flow. The clinical isolates A-26 (*ica*$^+$, biofilm^c) and A-10 (*ica*$^+$, biofilm$^-$) displayed PIA-based biofilm formation phenotypes under flow that were similar to those of 35984 and 12228, respectively. A-26 displayed an ~100-fold increase in PIA matrix over all shear stresses after only 12 h of shear, whereas A-10 was unable to form biofilms after 24 h (Fig. 3A). Both of these strains contain an intact *ica* locus; however, they display drastically different PIA-based biofilm formation phenotypes in both static and flow culture.

Fluid shear induces PIA-positive biofilm formation. Unexpectedly, upon exposure to fluid flow and shear (instead of ethanol, the usual inducer), strain A-5 (*ica*$^+$, biofilm^i) formed significant PIA biofilms (Fig. 3B and D). After 12 h of exposure to fluid flow, A-5 had viable cells on the channel surface (Fig. 3E) but displayed no significant change in PIA secretion (Fig. 3B). However, after this initial lag phase, there was significant production at 24 h of culture and 0.265 Pa (Fig. 3B) compared to that of A-10 (biofilm$^-$) ($P < 0.005$).

Other ethanol-inducible strains (W-166 and Z-173) also formed PIA biofilms when exposed to fluid shear alone. These strains formed biofilms across a broader spectrum of shear stresses than did A-5 (Fig. 3C; see also Fig. S3C and D in the supplemental material), resulting in larger biofilms at higher shear ($P < 0.03$). Interestingly, in comparison with A-5, successful biofilm formation at higher shears in these strains corresponded to a stronger induction by ethanol in microtiter plates (see Fig. S3B in the supplemental material).

Further investigation of fluid flow-mediated biofilm formation in A-5 revealed a biphasic dependence on shear stress. Quantification of the fold increase in secreted PIA matrix showed that at a low enough shear (0.016 Pa), A-5 cultures no longer yielded WGA signals that were significantly different from those of the PIA-negative control (A-10) at 0.167 Pa ($P > 0.25$). This result is also consistent with the fact that A-5 does not form biofilm in static culture. Notably, as observed for A-10 (Fig. 4C), the inability to secrete PIA does not prevent cells from adhering to the channel surface, as there were still viable cells in the channel following 24 h of culture.

Fluid shear induces PIA-positive biofilm formation rather than selecting for preexisting mutants. Our results suggested that PIA secretion in A-5 was a result of fluid shear; however, it was unclear if this was induction of a phenotype or selection of a low-frequency preexisting mutant genotype. To address this question,

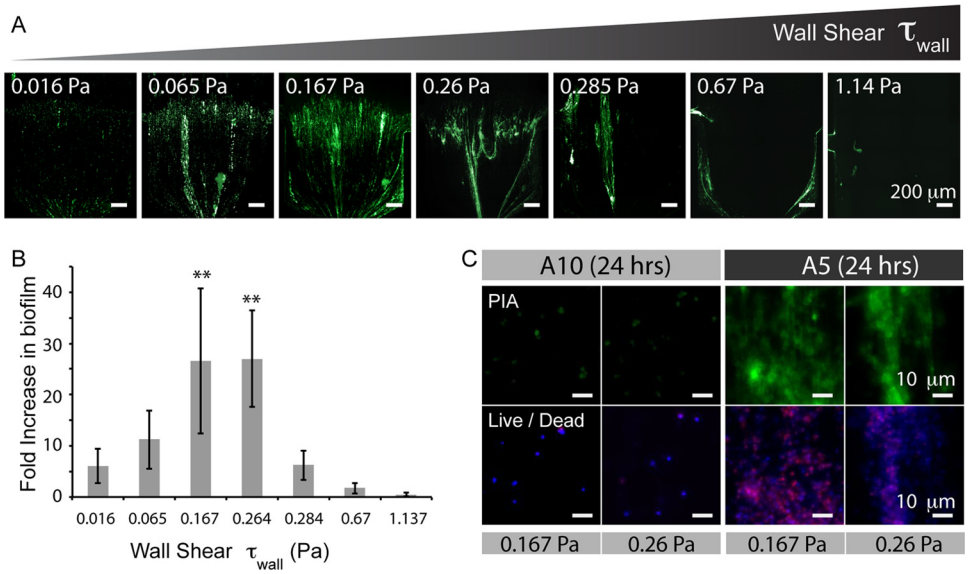

FIG 4 The formation of biofilms under flow by strain A-5 has a biphasic dependence on shear. (A) Stitched images with a ×20 magnification of WGA-stained A-5 biofilms across a broad range of shear stresses. Images are representative of each shear stress value, using devices with two inlet flow rates of 18 μl/min and 4.5 μl/min. (B) Quantification of the fold increase in biofilm in panel A. (C) Images with ×40 magnification of both the PIA matrix and live and dead cells. The panels for A-10 after 24 h show the presence of live cells on the channel surface, indicating that not all of the cells unable to form biofilm are washed out of the chamber during flow. **, $P < 0.05$, measured against the value of A-5 at 0.016 Pa. Green, PIA; blue, DAPI; red, EtHDI.

we harvested biofilms from the device to characterize their induction by EtOH without flow.

Cells from shear-induced biofilms that were excised from the device maintained the wild-type A-5 phenotype in microtiter plate assays. Six clones from 2 separate devices were harvested from the channels after exposure to conditions resulting in induction (0.167 Pa) and assayed in microtiter plate format. Each clone, secreting significant PIA under shear, was unable to form biofilms when grown in medium without flow, and all were induced to form biofilms with the addition of 2% and 4% EtOH, showing no significant difference from the wild type (Fig. 5D and E; see also Fig. S4 in the supplemental material). Further, assaying A-5 in a device at very low shear stresses (0.0045 Pa) resulted in no statistical difference ($P > 0.25$) from A-5 grown without flow (Fig. 5A to C) in terms of PIA matrix per cell area, and this readout increased with increasing shear stress in our device ($P < 0.01$).

DISCUSSION

The fluid flow microenvironment plays a significant role in the production and architecture of *S. epidermidis* PIA-positive biofilms. Table 1 summarizes the biofilm formation phenotypes of the *S. epidermidis* strains tested in this study under normal culture conditions as well as under ethanol stress and fluid shear. In strains constitutively producing PIA, the presence of fluid shear results in the formation of biofilm streamers, with higher shear leading to faster streamer formation. These structures were likely a result of the local fluid flow environment, as "streamers" in *Pseudomonas aeruginosa* have been observed by Rusconi et al. to be influenced by local fluid streamlines in curving flows (18, 19).

After 12 h of culture, markedly different PIA matrix structures with more-homogenous and dense matrices at lower shear and complex web-like structures at higher shear formed. This may have important implications concerning the potential of these strains to cause infection and their susceptibility to antimicrobial treatments, the effectiveness of which can be reduced by altered metabolic profiles in the biofilm (20, 22).

A correlation between microtiter plates and microfluidic devices showed that PIA is the main matrix component for the strains used in this study. Microtiter plates detected biofilms irrespective of matrix composition. In contrast, staining in the microfluidic device was specific for the PIA matrix. If strains were observed to be biofilm$^+$ in microtiter plates and biofilm$^-$ in the microfluidic device, this would indicate that PIA was not the main component. This was not the case in our experimental conditions, showing that PIA is the main matrix molecule.

Most importantly, we have demonstrated that clinical strains of *S. epidermidis* shown to produce biofilms when exposed to alcohols (A-5, W-166, and Z-173) are also induced to secrete PIA when exposed to fluid shear alone. Specifically, for strain A-5, we have shown no significant PIA to be present at very low to no fluid shear, whereas PIA matrix production increases significantly with increasing shear stress. This trend was observed when considering either total PIA or the PIA matrix normalized by the number of cells present in each measurement. Second, we show that the same cells that produce significant PIA under flow revert to a wild-type phenotype when excised from the device and grown in microtiter plates. This strongly supports the hypothesis that PIA production is induced by the environment rather than by selection of a stochastically arising subpopulation of cells that were expressing high levels of PIA and potentially would stick better to the substrate.

Previously, Yarwood et al. have shown that *agrD* mutants in *Staphylococcus aureus* form stronger biofilms than the wild type when grown under static culture; however, no differences were observed when grown under flow (24). We hypothesize that this may result from fluid flow washing away soluble quorum-sensing molecules, mimicking the environment created by an Δ*agrD* background. From our results and these previous data, we specu-

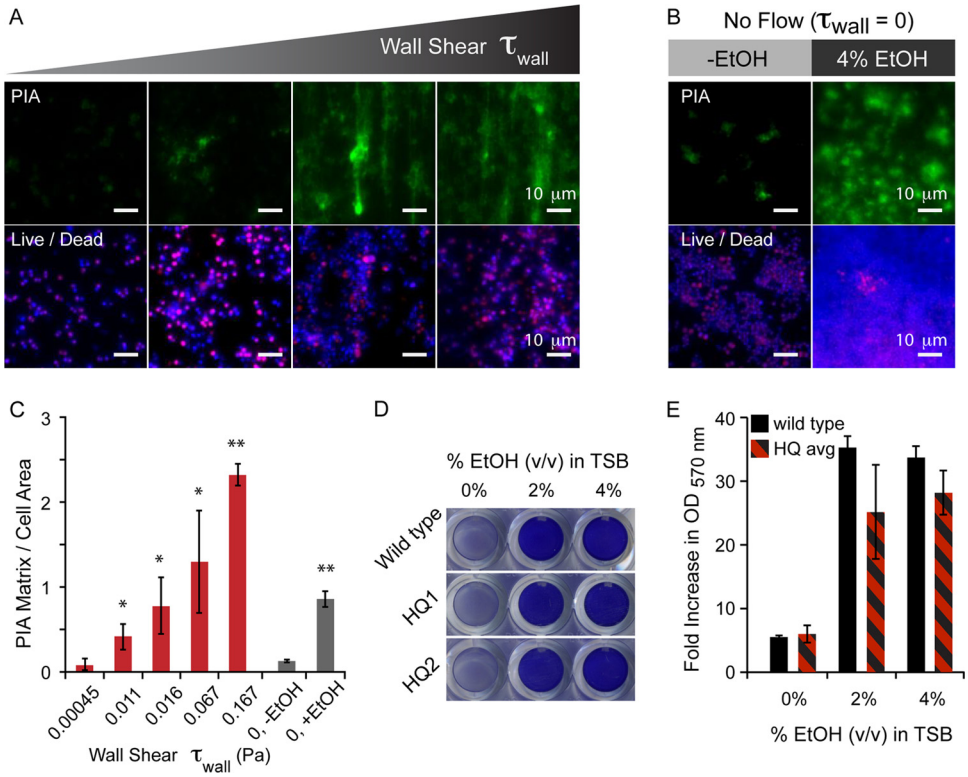

FIG 5 Fluid flow and shear induce the formation of biofilms in *S. epidermidis* A-5. (A) Images with ×40 magnification showing increased PIA matrix deposition with increasing wall shear in low-flow-rate regimes. Bottom panels show the presence of live cells on the surface, even when no visible matrix is present. (B) Images with ×40 magnification from no-flow controls in PDMS/glass wells, showing increased PIA matrix upon EtOH induction. There are live cells present in both cases. (C) Quantification of the ×40-magnified images from panels A and B, presented as the PIA matrix normalized to the area of the cells present. The ratio of the PIA matrix to cell area increases with increasing wall shear and also with increasing EtOH without fluid shear. (D) Representative images of microtiter plate assay screening clones isolated from the microfluidic biofilm assay. HQ1 and HQ2 are clones collected from independent flow-induced biofilms. (E) Quantification of the absorbance of microtiter plate assays at 570 nm. Black bars are the wild type, and the black/red bars are the averages of six clones collected from two separate flow experiments. One asterisk indicates a *P* value of <0.05 and two asterisks indicates a *P* value of <0.01 measured against respective minimum values.

late that fluid flow induction may occur through two mechanisms: (i) mechanical sensing of fluidic forces at the cellular level and/or (ii) quorum-sensing dysregulation by convective transport of soluble molecules away from cells.

Regardless of the mechanism, the induction of PIA-positive biofilms in *S. epidermidis* by fluid shear is strain dependent, enabling bacteria that do not produce biofilms under static conditions to increase their pathogenicity by secreting PIA, solely due to experiencing fluid shear. This is particularly relevant as the fluid shear stresses we have shown to induce PIA secretion are present in catheters under normal operating conditions. Our results warrant further investigation into the molecular mechanisms involved in the regulation of biofilm formation as well as a reconsideration of catheter luminal designs and operation with mechanical forces in mind.

TABLE 1 Phenotypes of *S. epidermidis* biofilm formation under ethanol stress and fluid shear

Strain	Source	Genotype	Phenotype	Biofilm production in:		
				TSB alone	EtOH	Fluid shear
12228	ATCC	Lacking *ica*	No biofilm	−	−	−
35984	ATCC	*ica*$^+$	Constitutive	+	+	+
A-26	13	*ica*$^+$	Constitutive	+	+	+
A-10	13	*ica*$^+$	No biofilm	−	−	−
A-5	13	*ica*$^+$	Inducible	−	+	+
W-166	13	*ica*$^+$	Inducible	−	+	+
Z-173	13	*ica*$^+$	Inducible	−	+	+

ACKNOWLEDGMENT

This work was supported in part by a 2010 Stein Oppenheimer Endowment Award (to V.M.).

REFERENCES

1. **Conlon KM, Humphreys H, O'Gara JP.** 2002. *icaR* encodes a transcriptional repressor involved in environmental regulation of *ica* operon expression and biofilm formation in *Staphylococcus epidermidis*. J. Bacteriol. **184**:4400–4408.
2. **Dice B, et al.** 2009. Biofilm formation by ica-positive and ica-negative strains of Staphylococcus epidermidis in vitro. Biofouling **25**:367–375.
3. **Dimick JB, et al.** 2001. Increased resource use associated with catheter-related bloodstream infection in the surgical intensive care unit. Arch. Surg. **136**:229–234.
4. **Fey PD, Olson ME.** 2010. Current concepts in biofilm formation of Staphylococcus epidermidis. Future Microbiol. **5**:917–933.
5. **Firrell JC, Lipowsky HH.** 1989. Leukocyte margination and deformation in mesenteric venules of rat. Am. J. Physiol. **256**:H1667–H1674.
6. **Heilmann C, et al.** 1996. Molecular basis of intercellular adhesion in the biofilm-forming Staphylococcus epidermidis. Mol. Microbiol. **20**:1083–1091.

7. **Knobloch JK, et al.** 2001. Biofilm formation by *Staphylococcus epidermidis* depends on functional RsbU, an activator of the *sigB* operon: differential activation mechanisms due to ethanol and salt stress. J. Bacteriol. **183**:2624–2633.
8. **Knobloch JK-M, Horstkotte MA, Rohde H, Kaulfers P-M, Mack D.** 2002. Alcoholic ingredients in skin disinfectants increase biofilm expression of Staphylococcus epidermidis. J. Antimicrob. Chemother. **49**:683–687.
9. **Lipowsky HH, Kovalcheck S, Zweifach BW.** 1978. The distribution of blood rheological parameters in the microvasculature of cat mesentery. Circ. Res. **43**:738–749.
10. **Mack D, et al.** 1996. The intercellular adhesin involved in biofilm accumulation of *Staphylococcus epidermidis* is a linear β-1,6-linked glucosaminoglycan: purification and structural analysis. J. Bacteriol. **178**:175–183.
11. **Milisavljevic V, Tran LP, Batmalle C, Bootsma HJ.** 2008. Benzyl alcohol and ethanol can enhance the pathogenic potential of clinical Staphylococcus epidermidis strains. Am. J. Infect. Control **36**:552–558.
12. **Qin Z, et al.** 2007. Formation and properties of in vitro biofilms of ica-negative Staphylococcus epidermidis clinical isolates. J. Med. Microbiol. **56**:83–93.
13. **Rohde H, Knobloch JK, Horstkotte MA, Mack D.** 2001. Correlation of biofilm expression types of Staphylococcus epidermidis with polysaccharide intercellular adhesin synthesis: evidence for involvement of icaADBC genotype-independent factors. Med. Microbiol. Immunol. **190**:105–112.
14. **Rohde H, et al.** 2005. Induction of Staphylococcus epidermidis biofilm formation via proteolytic processing of the accumulation-associated protein by staphylococcal and host proteases. Mol. Microbiol. **55**:1883–1895.
15. **Rosenthal VD, et al.** 2008. International Nosocomial Infection Control Consortium report, data summary for 2002-2007, issued January 2008. Am. J. Infect. Control **36**:627–637.
16. **Rupp ME, Ulphani JS, Fey PD, Bartscht K, Mack D.** 1999. Characterization of the importance of polysaccharide intercellular adhesin/hemagglutinin of *Staphylococcus epidermidis* in the pathogenesis of biomaterial-based infection in a mouse foreign body infection model. Infect. Immun. **67**:2627–2632.
17. **Rupp ME, Ulphani JS, Fey PD, Mack D.** 1999. Characterization of *Staphylococcus epidermidis* polysaccharide intercellular adhesin/hemagglutinin in the pathogenesis of intravascular catheter-associated infection in a rat model. Infect. Immun. **67**:2656–2659.
18. **Rusconi R, Lecuyer S, Autrusson N, Guglielmini L, Stone HA.** 2011. Secondary flow as a mechanism for the formation of biofilm streamers. Biophys. J. **100**:1392–1399.
19. **Rusconi R, Lecuyer S, Guglielmini L, Stone HA.** 2010. Laminar flow around corners triggers the formation of biofilm streamers. J. R. Soc. Interface **7**:1293–1299.
20. **Schaible B, Taylor CT, Schaffer K.** 2012. Hypoxia increases antibiotic resistance in *Pseudomonas aeruginosa* through altering the composition of multidrug efflux pumps. Antimicrob. Agents Chemother. **56**:2114–2118.
21. **Uçkay I, et al.** 2009. Foreign body infections due to Staphylococcus epidermidis. Ann. Med. **41**:109–119.
22. **Walters MC, Roe F, Bugnicourt A, Franklin MJ, Stewart PS.** 2003. Contributions of antibiotic penetration, oxygen limitation, and low metabolic activity to tolerance of *Pseudomonas aeruginosa* biofilms to ciprofloxacin and tobramycin. Antimicrob. Agents Chemother. **47**:317–323.
23. **Weaver WM, Dharmaraja S, Milisavljevic V, Di Carlo D.** 2011. The effects of shear stress on isolated receptor-ligand interactions of Staphylococcus epidermidis and human plasma fibrinogen using molecularly patterned microfluidics. Lab Chip **11**:883–889.
24. **Yarwood JM, Bartels DJ, Volper EM, Greenberg EP.** 2004. Quorum sensing in *Staphylococcus aureus* biofilms. J. Bacteriol. **186**:1838–1850.